

MR properties of excised neural tissue following experimentally induced demyelination

Ewa E. Odrobina,¹ Toby Y. J. Lam,¹ Teresa Pun,¹ Rajiv Midha^{2,3} and Greg J. Stanisz^{1,4*}

¹Imaging Research, Sunnybrook and Women's College Health Science Centre, Toronto, Ontario, Canada

²Neuroscience Research and Division of Neurosurgery, Sunnybrook & Women's College Health Science Centre, Toronto, Ontario, Canada

³Department of Surgery, University of Toronto, Toronto, Ontario, Canada

⁴Department of Medical Biophysics, University of Toronto, Toronto, Ontario, Canada

Received 12 October 2004; Revised 29 November 2004; Accepted 6 December 2004

ABSTRACT: Changes in the magnetic resonance (MR) parameters of demyelinated neural tissue were measured *in vitro* using an experimental animal model. A tellurium (Te) diet was applied to weanling rats to induce the demyelination process in the sciatic nerve. The quantitative MR parameters, such as T_1 , T_2 relaxation time constants and magnetization transfer (MT) were measured each day after applying the Te diet (up to 7 days) and were found to be substantially different from those of normal nerves. An increase in the average T_1 and T_2 was observed along with a decrease in the MT ratio (MTR) and the quantitative MT parameter M_{0B} , which describes the semisolid pool of protons. Most of the MR parameters correlated very well with the myelin fraction of neural tissue evaluated by quantitative histopathology. The T_2 relaxation spectrum provided the most efficient quantitative assessment of changes in neural tissue microstructure and its analysis resulted in a powerful tool to distinguish the processes of demyelination and inflammation. In comparison, the MT measurements were less successful. Copyright © 2005 John Wiley & Sons, Ltd.

KEYWORDS: demyelination; rat sciatic nerve; Te; MRI; magnetization transfer; T_1 ; T_2 ; MTR

INTRODUCTION

Myelin content is commonly used as an indicator of nerve health since the demyelination process is often associated with neural pathology such as multiple sclerosis (MS),^{1,2} trauma³ and dementia.⁴ Since demyelination often occurs concurrently with inflammation and axonal loss, distinguishing the pure demyelination processes from inflammation or tissue degeneration is challenging. The situation is even more complicated because similar qualitative changes in the MR signal intensities in the T_1 , T_2 or magnetization transfer (MT) weighted images are observed in these processes.^{5,6} It is of great importance to establish MRI protocols that are capable of differentiating and quantitative assessment of these pathologies. MRI as a non-invasive method could help in obtaining

accurate diagnosis and in evaluating the efficacy of various treatments.

Quantitative MR measurements are thought to provide more specific information about changes in tissue microstructure. For example, quantitative T_2 and MT measurements have been proposed as a proper method for myelin evaluation.^{7–10} Both methods are capable of measuring certain aspects of water molecular dynamics. However, it has been proposed that multi-component T_2 analysis provides more direct measure of myelin content in the nervous system.⁹ The observed, short T_2 component, which occurs at approximately 10–20 ms, has been associated with water in the myelin sheath,¹⁰ and thus provides a measure of the processes of demyelination and remyelination. We have already demonstrated that the magnitude of the short T_2 component correlates very well with the amount of myelin in nerves undergoing degeneration and spontaneous regeneration following traumatic injury of the peripheral nervous system (PNS).¹¹

The goal of this study was to evaluate experimentally how the process of demyelination alone influences the MR parameters and to determine whether it is possible to differentiate between demyelination and inflammation by MR. For this purpose we used an experimental, animal model of neural tissue demyelination by applying a tellurium (Te) diet for weanling rats.^{12–14} The toxicity of tellurium primarily induces segmental demyelination

*Correspondence to: G. J. Stanisz, Imaging Research, Sunnybrook & Women's College Health Science Centre, S654, 2075 Bayview Avenue, Toronto, Ontario, Canada M4N 3M5.

E-mail: stanisz@sten.sunnybrook.utoronto.ca

Contract/grant sponsor: Centre for Research Using Magnetic Resonance (CIHR); Contract/grant numbers: MOP57894, MMMES4182.

Abbreviations used: CAIA, computer-assisted image analysis; CPMG, Carr–Purcell–Meiboom–Gill sequence; EM, extracellular volume fraction; MT, magnetization transfer; MTR, magnetization transfer ratio; NNLS, used non-negative least-squares; PD, post-natal day; PNS, peripheral nervous system; Te, tellurium; WD, Wallerian degeneration.

in the sciatic nerve with negligible inflammation and axonal loss. The MR parameters were compared with the histomorphometric evaluation of intact or slightly degenerating myelin in the samples. Based on these findings, literature^{12–14} and our previous results on inflammation/demyelination processes,^{3,11,15} we were able to distinguish between these two processes, using the differences in the short component of the T_2 spectrum.

MATERIALS AND METHODS

Experimental model of demyelination

Several investigators have reported^{12–14,16} that weanling rats fed a Te diet exhibit paralysis of the hind limbs, which is attributed to segmental demyelination of the axons in the sciatic nerve. Te produces demyelination via metabolic alteration in the myelinating Schwann cells,¹⁷ rather than direct damage to the myelin sheath.¹⁴ Segmental demyelination was further visualized in work done by Duckett *et al.*,¹³ in which teased fiber studies revealed a periodic reduction in the myelin sheath that occurred along the length of the fiber. Bouldin *et al.*¹⁴ also reported nodal gaps wider than 10 μm following Te treatment, which is indicative of segmental demyelination. It was also reported¹⁸ that less than 2% of fibers undergo Wallerian degeneration suggesting that axons are minimally impacted by Te. These findings propose that the tellurium model of primary demyelination with minimal axonal degeneration can be used to examine the pure demyelination effect on MR parameters. We measured the MR properties of rat sciatic nerve *in vitro* after 1–7 days of applied Te diet. For each day we used seven samples with Te diet and five untreated samples as a control.

Weanling Lewis rats, post-natal day (PD) 11 were obtained from Charles River Canada (St Constant, QC, Canada). Animals were housed in a standard animal facility with a 12:12 light–dark cycle. Litters (including the dam) were housed in flat-bottom beta-chip lined cages and allowed *ad libitum* standard rat chow (1/2 inch pellets) and water. The rats were acclimatized for 6 days prior to the onset of the study. All experiments and animal interventions adhered strictly to Canadian Council on Animal Care guidelines.

Beginning on PD 14, animals were weighed and assessed for facility of movement daily. Upon removal of the dam (PD 17), experimental animals received a diet containing 1.1 wt% elemental Te (1/2 inch pellets), obtained from Bio-Serv (Frenchtown, NJ, USA), *ad libitum*. Filter cage tops were employed to limit Te exposure. Following diet onset, animals were anesthetized daily with an intramuscular injection of 100 mg/kg ketamine hydrochloride (0.1 ml/100 g Rogarestic; Rogra-STB, Montreal, QC, Canada) and 10 mg/kg xylazine (20 mg/ml; Bayer, Etobicoke, ON, Canada) and nerve samples

were harvested for further MR studies. Control pups remained on the standard rat chow and were sacrificed at the same time points.

Following anesthesia, the sciatic nerves were exposed via bilateral gluteal and posterior thigh incisions. The entire lengths of the right and left sciatic nerves were extracted from the sciatic notch onwards. The middle section (approximately 1 cm in length) was reserved for MR analysis. To ensure continuity in the tissue pathology across the sample, the proximal and distal portions of the nerve were evaluated histopathologically.

Histopathology

Proximal and distal nerve sections were fixed by immersion in Universal fixative (40% formalin, 25% glutaraldehyde), post-fixed with osmium tetroxide and embedded in epon-araldite. They were then sectioned on an ultramicrotome (Sorvall MT6000, Kendro, Asheville, NC, USA; or Reichert-Jung Ultracut E, Leica Microsystems, Germany). For each distal and proximal portion of the nerve, two histopathological samples were obtained for histomorphometric assessment of the myelin content, axonal integrity and EM fraction. Toluidine blue was used to stain 1 μm -thick cross-sections for light microscopy.

Using an Olympus BX51 light microscope (Olympus America Inc., Melville, NY, USA) linked to an image analysis system (Image Pro Plus version 4.5, Media Cybernetics, Silver Spring, MD, USA), nerve cross sections were evaluated. Images were captured using a Cool Snap-Pro camera (Media Cybernetics Inc., Silver Springs, MD, USA) and axons larger than 0.5 μm in diameter were analyzed. The analysis involved a three-step approach modeled on the segmentation, recognition and measurement method of Romero *et al.*¹⁹ as previously developed in our laboratory.¹¹ Seven representative fields (3093 μm^2) at 1000 \times magnification were sampled per cross-section. This ensured that the total area evaluated was at least 25% of the total cross sectional area. Measurements of interest included both intact and slightly disrupted myelin sheaths. The myelin in the form of Wallerian degeneration (WD) profiles was not counted. The myelin content and extracellular matrix volume (EM) fraction were calculated as percentages of the total sampled area. Additionally, immuno-histologic evaluation of the inflammatory process (using antibodies for ED1, a macrophage and monocyte cytoplasmic antigen) was performed in order to evaluate the inflammatory response of Te. In all measured samples inflammation was not observed.

MR measurements

All MR measurements were performed at 20°C and 1.5 T on a 20 cm-bore superconducting magnet (Nalorac

Cryogenics Corp., Martinez, CA, USA) controlled by a SMIS spectroscopy console (SMIS, Surrey, UK). Rectangular radiofrequency (RF) pulses were amplified by an RF amplifier (model 3205; American Microwave Technology, Brea, CA, USA). Immediately after tissue excision, the samples were placed in non-protonated, MR-compatible fluid (Fluorinert; 3M, London, Canada) to avoid dehydration and to reduce susceptibility effects. The MR experiments lasted approximately 3 h. Before and after each experimental session, a multicomponent T_2 decay was measured using a Carr–Purcell–Meiboom–Gill (CPMG) sequence to test the continuity of the sample signal characteristics. The T_2 decay curves varied <1% during these sessions, which indicated that the samples were stable over the time-course of the MR experiments. Moreover, it has been found that the measured MR parameters were independent on the sample orientation with respect to the main magnetic field (B_0). This is to be expected, since there is no T_1 , T_2 or MT anisotropy in neural tissue.²⁰

The MR experimental session consisted of:

- T_1 relaxation time data were acquired using an inversion recovery (IR) sequence²¹ with 35 TI (inversion recovery time) values logarithmically spaced from 1 to 32 000 ms, with 10 s between each acquisition and the next inversion pulse, and two averages;
- T_2 relaxation time data were acquired using a standard CPMG sequence²² with TE/TR (echo time/repetition time) = 1/10 000 ms, 2000 even echoes sampled and 200 averages;
- MT-weighted data were measured using a continuous-wave (cw) saturation pulse of 7 s duration. For the standard MTR evaluation, the RF saturation pulse amplitude (rotational frequency $\omega_1/2\pi$) was 670 Hz, and the offset frequency of the saturation, Δ , was 5 kHz. To quantitatively evaluate the MT data,²³ four RF saturation amplitudes ($\omega_1/2\pi = 85, 170, 670$ and 2670 Hz) and 26 off-resonance frequencies Δ (14–250 kHz) were applied. The TR was 10 s, and the number of averages was eight. The effects of any residual transverse magnetization following the off-resonance irradiation was removed by phase-cycling the $\pi/2$ pulse ($-x/x$).

Data analysis

The T_1 data were analyzed assuming mono-exponential behavior. Our recent results¹⁵ show that this assumption is valid for a rat sciatic nerve.

All T_2 decay data were fitted to a multicomponent T_2 model in which the relaxation of each T_2 component had a Gaussian distribution on a logarithmic time scale.^{11,24} The Gaussian fitting procedure yielded values for the T_2 spectrum position, width, amplitude. The area under the Gaussian peak yielded the relative size of each compo-

nent. The Gaussian model was found to provide better separation of the T_2 peaks than the commonly used non-negative least-squares (NNLS) method,²⁵ yet guaranteed approximately the same value of χ^2 and resulted in similar T_2 spectra. Repeated T_2 measurements of a single sample were used to determine that a minimum signal-to-noise ratio (SNR), of 500 was required in order to assess the amplitudes and positions of all three T_2 components with 5% precision.

The MTR was evaluated by the following equation:

$$MTR = (M_o - M_{SAT})/M_o \quad (1)$$

where M_o and M_{SAT} denote signal amplitude measured without and with the RF saturation pulse, respectively.

The quantitative MT data were fitted to a ‘two-pool’ model²³ quantifying the exchange between an unrestricted liquid pool and a semisolid macromolecular pool of restricted mobility.²⁶ The model estimates R , the rate of exchange of longitudinal magnetization between liquid and semisolid pools, as well as the dimensionless parameters $1/R_A T_{2A}$ and RM_{OB}/R_A , where R_A is the rate constant of longitudinal relaxation in the liquid pool, T_{2A} is the average transverse relaxation time of the liquid pool, and M_{OB} is the fraction of magnetization that resides in the semisolid pool and undergoes MT exchange.

RESULTS

Histopathology

The histopathology results indicate the drastic changes in the rat sciatic nerve microstructure as a result of a tellurium diet. Figure 1 shows representative toluidine blue-stained sections of normal sciatic nerve [Fig. 1(a)] and nerves after 1 day [Fig. 1(b)], 4 days [Fig. 1(c)], and 7 days [Fig. 1(d)], on the Te diet. The normal sciatic nerve sample shows well-myelinated axons with adjacent nuclei consisting of mainly Schwann cells [Fig. 1(a)]. In the sciatic nerve following the Te diet, the process of demyelination with its consequent stages is clearly observed. For example, in the nerve 4 days following Te diet [Fig. 1(c)], it can be observed that not all axons are well myelinated. Some are surrounded by a much thinner myelin layer compared with a normal nerve. Additionally, a larger distribution in the axons’ diameters and an increasing distance between them (increased extracellular volume fraction, EM) is observed. In the image of the nerve following 7 days on the Te diet [Fig. 1(d)], the Wallerian degeneration profiles (arrows) and myelin debris (stars) were observed together with the significant axonal loss, indicating the advanced demyelination process. No substantial differences in histopathology between the proximal and distal nerve samples were observed, which indicates tissue uniformity across the intervening measured MR samples.

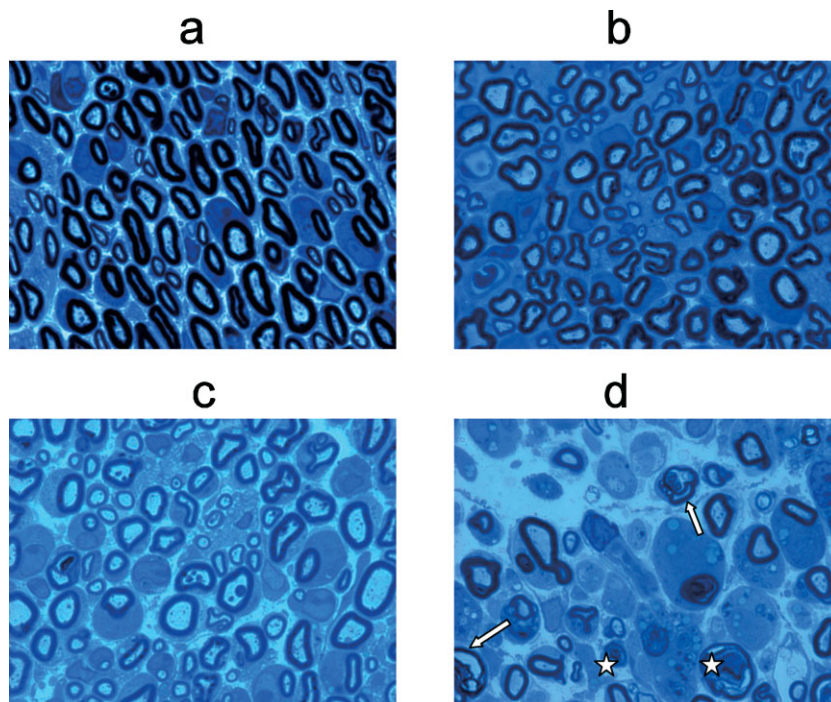


Figure 1. Toluidine blue-stained cross sections of nerves at $1000\times$ magnification. (a) Normal sciatic nerve sample. The axons are well myelinated, with the occasional Schwann cell present. (b) Sciatic nerve 1 day after Te diet. (c) Sciatic nerve 4 days after Te diet. Part of the axons is not as well myelinated as for the normal one. Additionally, larger distribution in axon's diameters and increasing distance between them (increased EM fraction) is observed. (d) Sciatic nerve 7 days after Te diet. The Wallerian degeneration profiles (arrows) and myelin debris (stars) are observed together with significant axonal loss, indicating the advanced demyelination process

We performed a quantitative assessment with computer-assisted image analysis (CAIA) on the toluidine blue-stained slides, which allowed us to estimate the myelin content and EM fraction (including myelin debris). In our calculations, we only counted intact myelin sheaths or slightly degenerated myelin. Myelin debris was not taken into account. The myelin content of the normal nerves was $28 \pm 3\%$, while for the Te diet treated samples it was significantly lower ($8 \pm 4\%$ for day 7 Te diet).

MR parameters

T_1 relaxation [Fig. 2(a)] appeared mono-exponential, for all measured samples, with the average longitudinal relaxation time T_1 equal to 675 ± 22 ms for untreated nerves. T_2 relaxation was multi-exponential, showing three well-distinguished T_2 components. Typical T_2 spectra for normal and Te diet treated nerves are shown in Fig. 2(b). The T_2 spectrum of normal nerve (solid line) shows three well-distinguished components (centered at short, intermediate, and long values of T_2) described as follows:

- a short T_2 component at 23 ± 3 ms (average and standard error of the mean for 35 samples) represented $28 \pm 4\%$ of the total curve area;

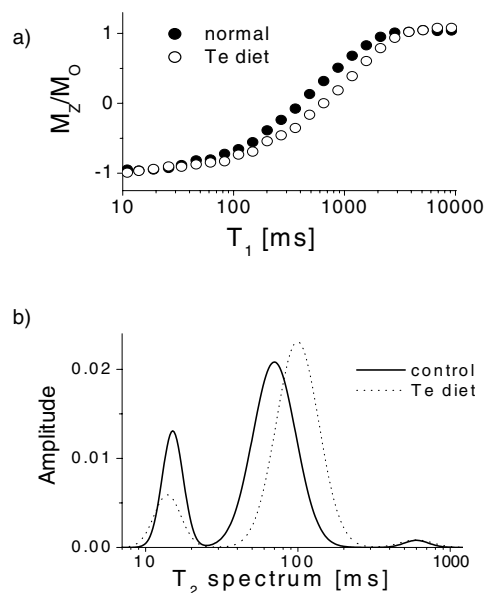


Figure 2. (a) An example of inversion recovery data. The abscissa is inversion time (T_1) on a logarithmic scale, causing the T_1 recovery to appear as a sigmoidal curve: solid circles (●) represent normal sample and open circles (○) represent sample after 4 days of tellurium (Te) diet. (b) T_2 spectrum

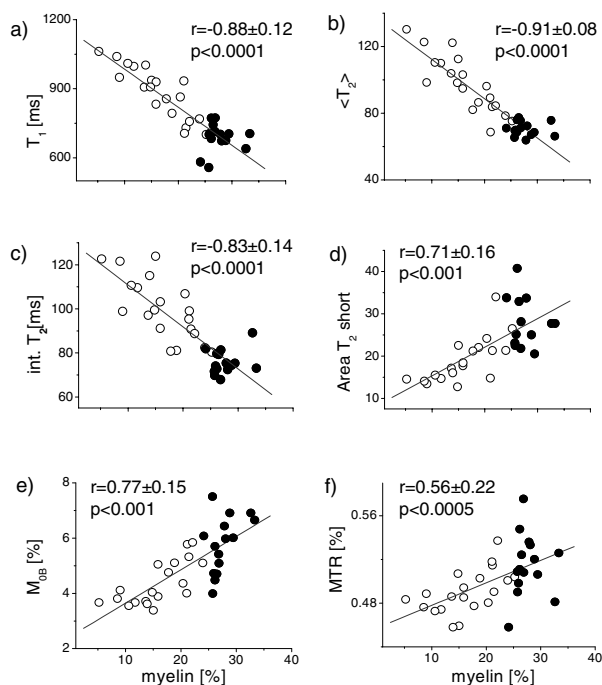


Figure 3. Correlation between the MR parameters and quantitative measure of the myelin fraction. Solid and open circles indicate controls and Te diet-treated samples, respectively: (a) T_1 relaxations; (b) the average T_2 , $\langle T_2 \rangle$; (c) the value of the intermediate T_2 component; (d) the area under the short T_2 component; (e) the MT semisolid pool fraction M_{0B} ; (f) MTR as a function of the myelin in the samples

- an intermediate T_2 component at 75 ± 4 ms, with size $74 \pm 4\%$ of the total curve area;
- a long T_2 component at 598 ± 3 ms, with size $1.5 \pm 0.5\%$ of the total curve area.

Moreover, the single measure of the T_2 relaxation, $\langle T_2 \rangle$, was evaluated. $\langle T_2 \rangle$ represents an average of the T_2 relaxation spectrum, and is equivalent to the mono-exponential estimate of T_2 decay that is usually assessed in clinical MRI. The $\langle T_2 \rangle$ average for the normal nerve was 69 ± 3 ms.

The MTR for normal nerves, measured at a saturation pulse amplitude, $\omega_1/2\pi$, of 670 Hz and offset frequency of the saturation, Δ , equal to 5 kHz, was 0.51 ± 0.02 . The two-pool MT model resulted in an MT exchange rate R of 57 ± 8 and a fraction of the semisolid pool M_{0B} equal to $6.3 \pm 0.4\%$.

Most of the MR properties of the Te diet-treated nerves were significantly different from the normal nerves. Figure 2 shows the T_1 data and T_2 relaxation spectrum for a normal nerve and a typical Te diet treated nerve after a few days of the diet. The T_1 relaxation time for the Te diet-treated samples increased with duration of the applied diet and reached the value of 1036 ± 37 ms after 7 days. The T_2 spectrum was also different and is described below:

- the short T_2 component position slightly moved towards shorter times in comparison to the normal nerve (19 ± 1 ms); however, its percentage of the total area significantly decreased with duration of Te diet up to $14 \pm 1\%$ [Fig. 2(b)];
- the intermediate peak position increased to 108 ± 3 ms, and its total area increased slightly to $83 \pm 1\%$;
- the long peak position practically did not change (594 ± 3 ms), but its percentage of the total area increased slightly to $2.8 \pm 0.6\%$.

The average $\langle T_2 \rangle$ relaxation time also increased and was equal to 109 ± 5 ms. The MT data also showed differences between normal and Te diet-treated nerves. The MTR was, on average, lower than that of normal nerves (0.47 ± 0.01). The semisolid pool M_{0B} decreased to $3.8 \pm 0.2\%$, whereas the MT exchange rate R remained the same at 57 ± 5 s $^{-1}$.

To assess whether the changes in the MR parameters mapped onto the observed changes in histopathology, we compared the MR parameters with the quantitative morphometric measure of myelin in the nerve samples. Figure 3 shows the T_1 (a); the average T_2 , $\langle T_2 \rangle$ (b); the value of the intermediate T_2 component (c); the area under the short T_2 component (d); the MT semisolid pool fraction M_{0B} (e); and the phenomenological measure of MT – MTR (f) as a function of the myelin fraction for all measured samples. The average relaxation times, T_1 and $\langle T_2 \rangle$, and the value of the intermediate T_2 component increased with the decrease of myelin fraction. The area under the short T_2 component, the MT semisolid fraction M_{0B} and the MTR decreased with the decrease of myelin fraction. Figure 3 illustrates the substantial correlation (as reflected in the correlation coefficient, r , between the measured MR parameters and the histomorphometric assessment of the myelin fraction. The errors represent uncertainties in r within a 95% confidence level. It is evident that most of the MR parameters were strongly correlated with histopathology.

DISCUSSION

From the histomorphometric results (Fig. 1) and literature^{12–14} we conclude that a Te diet in weanling rats is a good means of inducing the demyelination process with minimal axonal loss and inflammation for the first few days (in our case 4 days) of the diet. For longer duration times of the Te diet, significant axonal loss is observed [e.g. day 7, Fig. 1(d)], indicating, in contrast to the literature,^{12–18} substantial degeneration of neural tissue. The most pronounced changes in MR parameters in comparison to the controls were observed in the samples between 1 and 4 days of Te diet. During this time we observed primarily a demyelination process with minimal axonal damage and inflammation. Further maintaining the Te diet kept the changes in MR parameters growing,

but on average the difference between days 4 and 7 was moderate in comparison to the control and day 4.

Owing to variability in the histopathological results from Te treated samples, it was not feasible to make simple comparisons of the mean MR parameters across experimental conditions. Our primary focus was to examine whether the variability in histopathology correlated with the MR measurements. In animal models of disease, it is common that the degree of tissue damage is variable across different animals.¹¹ For this reason, instead of comparing the Te-treated samples with the controls, we compared the MR measurements for each individual sample to the histopathological results. The current results demonstrate that standard MR techniques, such as average T_1 , T_2 relaxation and MTR, correlate strongly with demyelination and are consistent with observed MRI of a variety of neural system pathologies.

The experimental data presented here describe *ex vivo* nerve tissue measured at room temperature. Therefore, it is not expected that the extracted MR parameters will have exactly the same values for *in vivo* neural tissue. T_1 , T_2 relaxation times and inter-compartmental exchange all increase with temperature.²⁷ However, qualitatively, the MR properties of *in vivo* tissue are not vastly different from those of excised tissue. In particular, the T_2 spectra of *in vivo* normal nerves are similar to those obtained in this study.^{28,29} Similarly, the quantitative MT parameters for *in vivo* neural tissue⁸ are comparable to those obtained *in vitro*.²⁶ Thus, it is difficult to believe that *in vivo* MR measurements will not exhibit similar changes in MR parameters as a result of demyelination.

The qualitative comparison between measured MR parameters and histopathology shows that most of the MR parameters are sensitive to demyelination and may be used as semi-quantitative evaluation of the degree of demyelination. For example, on average, the T_1 relaxation time increased by approximately 39% for day 4 and 58% for day 7 of the Te diet, whereas the T_2 relaxation time increased by 58% for day 4 of Te diet and stayed nearly unchanged up to day 7. The change in MTR was small (approximately 5%). The changes in more qualitative MR measures, such as the relative curve area of the T_2 short component (a 50% decrease), the value of the intermediate T_2 component (a 50% increase) and the MT macromolecular fraction, M_{OB} (a 38% decrease), were also pronounced. The MT exchange rate R appeared to be independent of demyelination. The moderate change in MTR due to demyelination may be explained by conflicting contributions of the MT and direct effects on the MTR. It has been shown that MTR is proportional to the RM_{OB}/R_A ratio.³⁰ In the case of demyelinated nerves, the decrease in MTR caused by decreased M_{OB} is counteracted by a decreased longitudinal relaxation rate, R_A .

The process of demyelination appears in most neural tissue diseases concurrently with axonal loss and inflammation. It is of great importance to differentiate between these processes to evaluate the characteristics of a given

neural disorder. This kind of diagnosis would help in assessing the proper response to therapeutic response. For example, we have shown that rat sciatic nerves that can spontaneously regenerate following traumatic injury are on average more inflamed than those with irreversible structural changes.¹¹ However, it is very difficult to distinguish between myelin loss and inflammation using standard MR techniques. In both cases, the changes in the MR signal intensities in the standard (clinically used) T_1 , T_2 and MT-weighted images are very similar. In our previous work¹⁵ we analyzed the changes in MR parameters following a pure inflammation process by applying pro-inflammatory cytokine tumor necrosis factor- α (TNF- α). Now we would like to compare this data with our present results—MR parameters characterizing the process of myelin loss alone. At first glance, both processes show similar increase in T_1 and T_2 relaxation times and decrease in the MT parameters. However, the changes in the T_2 spectrum during the demyelination process are significantly different from those taking place during inflammation. Figures 3(d) and 1(b) show that the area under the short T_2 component correlates nicely with the demyelination process and its decrease (in our case up to 50%) indicates the loss of myelin in the sample. In the case of an inflamed sample, the area under the short T_2 component only slightly decreases and does not correlate with the myelin content.¹⁵ It should be mentioned here that the MR experiment evaluates myelin content as a volume fraction of water in myelin, rather than the intra- and extracellular water volumes. Therefore, the process of inflammation, which results in the increase of fraction of extracellular water volume, will produce a decrease in the relative amplitude of the short T_2 component even if there is no myelin loss. However, this decrease in the relative amplitude of the short T_2 component is small in comparison to the case of demyelination. Summarizing these results, the model of occurring changes in T_2 spectrum of healthy nerve undergoing pure demyelination [Fig. 4(a)], pure inflammation [Fig. 4(b)] and combined processes of demyelination with axonal loss [Fig. 4(c)] was proposed.

In the case of pure demyelination, the loss of myelin induces a decrease in the short component of the T_2 spectrum, which is correlated to the amount of myelin in the nerve. A decrease in the short T_2 component causes the relative increase in the amplitude of the intermediate T_2 component [Fig. 4(a)], which results in overall increase in the $\langle T_2 \rangle$ value. In the pure inflammation process [Fig. 4(b)], the increase in the $\langle T_2 \rangle$ value is due to a significant shift in the intermediate T_2 peak towards longer relaxation times. This is because of an increase in extracellular volume due to swelling and the existence of inflammatory cells. The decrease in the short T_2 component is relatively small. Finally, considering the combined processes of demyelination and axonal loss at the same time [Fig. 4(c)], we deal both with the loss of myelin itself (decrease in the short T_2 component) and the

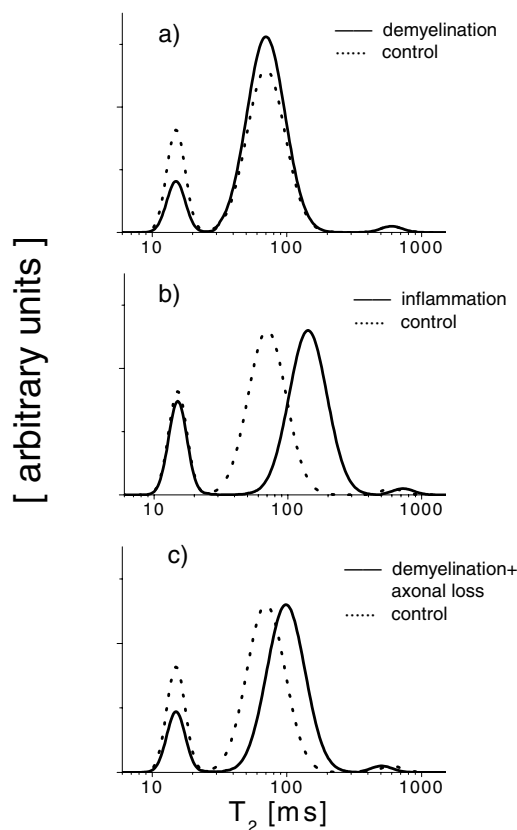


Figure 4. The model of changes in T_2 spectrum of nerve tissue for: (a) pure demyelination; (b) pure inflammation; (c) advanced nerve degeneration following both demyelination and axonal loss

increase in extracellular volume fraction due to loss of axons (shift of the intermediate T_2 peak towards longer relaxation times). However, this shift is not as significant as with inflamed tissue, as shown in Fig. 4(c).

It is interesting that our results indicate that in sciatic nerve MT measurements are not able to differentiate between the process of demyelination and inflammation. It is assumed that MT mainly measures the interactions that occur between water and protons associated with myelin lipids and, consequently, should be a perfect measure of the process of demyelination. The change in M_{0B} , which is the relative measure of the macromolecular proton population that takes an active part in the MT process and is defined as a fraction of the semisolid pool in comparison to that of liquid water, decreases about 40% and drops from 6.3% for the control sample to 2.8% for demyelinated sample. In the case of pure inflammation process, the M_{0B} unexpectedly decreases even more, to 50%.

In our previous work on the behavior of MR parameters in white matter (WM),⁹ we showed how the demyelination process should influence the MR parameters based on a theoretical model of two exchanging liquid pools, which well describes the experimental results in healthy optic nerve. These findings show that

a total loss of myelin in WM should result in a T_1 relaxation increase of approximately 20% and an average T_2 increase of 30%. In our case the change in both relaxation times T_1 and T_2 is larger and exceeds 50%. The model, however, predicts the general behavior of MR parameters well, including a decrease in the amplitude of the short T_2 component with myelin loss. The model shows that the changes in the T_1 relaxation are caused mainly by decreased MT effect, whereas the increase in the T_2 component is caused primarily by the disappearance of the short T_2 component (associated with myelin loss). Additionally, for total myelin loss in WM, the model predicts significant decrease in the semisolid macromolecular pool, M_{0B} , to $\sim 2\%$. This result also correlates with our findings for the sciatic nerve where, with the significant decrease of myelin, the M_{0B} semisolid macromolecular pool decreases from 6.3 to 3.8%. The largest discrepancy between the proposed model and the results of this paper can be observed for the MTR parameter. From the theoretical predictions of the model, the observed change in the MTR parameter should be about 30% for our case. The experiment, however, shows a decrease in the MTR of only 8%. This can be caused by the fact that the model neglects the process of axonal loss, which is present in the rats treated with the Te diet.

CONCLUSIONS

Most MR parameters change significantly in the presence of neural tissue demyelination. The area under the T_2 short component of the T_2 relaxation measurements is the best means of distinguishing between the process of the myelin loss and inflammation. The quantitative measurement of MT is less successful.

REFERENCES

- Moore G. MRI-clinical correlations: more than inflammation alone—what can MRI contribute to improve the understanding of pathological processes in MS? *J. Neurol. Sci.* 2003; **206**: 175–179.
- Gareau PJ, Rutt BK, Karlik SJ, Mitchell JR. Magnetization transfer and multicomponent T_2 relaxation measurements with histopathologic correlation in an experimental model of MS. *J. Magn. Reson. Imag.* 2000; **11**: 586–595.
- Stanisz GJ, Midha R, Munro CA, Henkelman RM. MR properties of rat sciatic nerve following trauma. *Magn. Reson. Med.* 2001; **45**: 415–420.
- Stoppe G, Staedt J, Brunhn H. Resonance-imaging value for the (differential) diagnosis of dementia of the Alzheimer-type and vascular dementia. *Fortschr. Neurol. Psychol.* 1995; **63**: 425–440.
- Harrison R, Bronskill MJ, Henkelman RM. Magnetization transfer and T_2 relaxation components in tissue. *Magn. Reson. Med.* 1995; **33**: 490–496.
- Does MD, Beaulieu C, Allen PS, Snyder RE. Multi-component T_1 relaxation and magnetisation transfer in peripheral nerve. *Magn. Reson. Imag.* 1998; **16**: 1033–1041.
- Pike GB, de Stefano N, Narayanan S, Francis GS, Antel JP, Arnold DL. Combined magnetization transfer and proton spectroscopic imaging in the assessment of pathologic brain lesions in multiple sclerosis. *Am. J. Neuroradiol.* 1999; **20**: 829–837.

8. Sled JG, Pike GB. Quantitative imaging of magnetization transfer exchange and relaxation properties *in vivo* using MRI. *Magn. Reson. Med.* 2001; **46**: 923–932.
9. Stanisz GJ, Kecojevic A, Bronskill MJ, Henkelman RM. Characterizing white matter with magnetization transfer and T_2 . *Magn. Reson. Med.* 1999; **42**: 1128–1136.
10. MacKay AL, Whittall KP, Adler J, Li DKB, Paty DW, Graeb D. *In vivo* visualisation of myelin water in brain by magnetic resonance. *Magn. Reson. Med.* 1994; **31**: 673–677.
11. Webb S, Munro CA, Midha R, Stanisz GJ. Is multicomponent T_2 a good measure of myelin content in peripheral nerve? *Magn. Reson. Med.* 2003; **49**: 638–645.
12. Lampert P, Garro F, Pentsche A. Tellurium neuropathy. *Acta Neuropathol.* 1970; **15**: 308–317.
13. Duckett S, Said G, Streletz LG, White RG, Galle P. Tellurium-induced neuropathy: correlative physiological, morphological and electron microprobe studies. *Neuropathol. Appl. Neurol.* 1979; **5**: 265–278.
14. Bouldin TW, Samsa G, Earnhardt TS, Krigman MR. Schwann cell vulnerability to demyelination is associated with internodal length in tellurium neuropathy. *J. Neuropathol. Exp. Neurol.* 1988; **47**: 41–47.
15. Stanisz GJ, Webb S, Munro CA, Pun T. MR Properties of neural tissue following experimentally induced inflammation. *Magn. Reson. Med.* 2004; **51**: 473–479.
16. Garro F, Pentsche A. Hydrocephalus internus in offspring of rats fed non-toxic amounts of tellurium during pregnancy. *J. Neuropathol. Exp. Neurol.* 1965; **24**: 137–147.
17. Harry GJ, Goodrum JF, Bouldin TW, Wagner-Reico M, Toews AD, Morell P. Tellurium-induced neuropathy: metabolic alterations associated with demyelination and remyelination in rat sciatic nerve. *J. Neurochem.* 1989; **52**: 938–945.
18. Said G, Duckett S. Tellurium-induced myelinopathy in adult rats. *Muscle Nerve* 1981; **4**: 319–325.
19. Romero E, Cuisenaire O, Deneff J, Macq B. Automatic morphometry of nerve histological sections. *J. Neurosci. Meth.* 2000; **97**: 111–122.
20. Henkelman RM, Stanisz GJ, Kim JK, Bronskill MJ. Anisotropy of NMR properties of tissues. *Magn. Reson. Med.* 1994; **32**: 592–601.
21. Carl H, Purcell E. Effects of diffusion on free precession in nuclear magnetic resonance experiments. *Phys. Rev.* 1954; **94**: 630–638.
22. Meiboom S, Gill S. Modified spin-echo method for measuring nuclear relaxation times. *Rev. Sci. Instrum.* 1958; **29**: 688–691.
23. Henkelman RM, Huang XM, Xiang QS, Stanisz GJ, Swanson SD, Bronskill MJ. Quantitative interpretation of magnetization transfer. *Magn. Reson. Med.* 1993; **29**: 759–766.
24. Stanisz GJ, Henkelman RM. Diffusional anisotropy of T_2 components in bovine optic nerve. *Magn. Reson. Med.* 1998; **40**: 405–410.
25. Whittall KP, MacKay AL. Quantitative interpretation of NMR relaxation data. *J. Magn. Reson.* 1989; **95**: 134.
26. Morrison C, Stanisz GJ, Henkelman RM. Modeling magnetization transfer for biological-like systems using a semi-solid pool with a super-Lorentzian lineshape and dipolar reservoir. *J. Magn. Reson. B* 1995; **108**: 103–113.
27. Stanisz GJ, Li JG, Wright GA, Henkelman RM. Water dynamics in human blood via combined measurements of T_2 relaxation and diffusion in the presence of gadolinium. *Magn. Reson. Med.* 1998; **39**: 223–233.
28. Does MD, Gore J. Compartmental study of T_1 and T_2 in rat brain and trigeminal nerve *in vivo*. *Magn. Reson. Med.* 2002; **47**: 274–283.
29. Laule C, Leung E, Li DK, Traboulsee AL, Paty DW, MacKay AL, Moore GW. Myelin water imaging in multiple sclerosis: quantitative correlation with histopathology, poster, F. ISMR, 2004.
30. Henkelman RM, Stanisz GJ, Graham SJ. Magnetization transfer in MRI: a review. *NMR Biomed.* 2001; **14**: 57–64.